RSC Advances

PAPER

View Article Online
View Journal | View Issue

Cite this: *RSC Adv.*, 2014, **4**, 13274

Rapidly dissolving poly(vinyl alcohol)/cyclodextrin electrospun nanofibrous membranes†

Joshua L. Manasco,‡ Christina Tang,‡§ Nancy A. Burns, Carl D. Saquing¶ and Saad A. Khan*

Received 22nd July 2013
Accepted 21st January 2014

DOI: 10.1039/c3ra43836h

www.rsc.org/advances

We electrospun supramolecular complexes of poly(vinyl alcohol) (PVA), hydroxypropyl-β-cyclodextrin (HPβCD), and a poorly water soluble model drug (ketoprofen) to produce moisture-sensitive fibers for potential sublingual drug delivery applications. Fast dissolving/disintegrating membranes are of particular importance in sublingual delivery of drugs and other functional moieties, and materials such as nanofibers with a high specific surface area may be well-suited for such applications. Surprisingly, the concentrations of PVA and HPβCD required to produce uniform blend fibers are lower than the respective neat components. We find that PVA plays a synergistic role in facilitating fiber formation, enabling us to produce fibers with a high cyclodextrin (*e.g.* 90 wt%) content. We attribute the mechanism of fiber formation to the presence of HPβCD aggregates and PVA chain networks, analogous to depletion flocculation. Fibers with the highest HPβCD content release the most drugs in the shortest amount of time, and the amount of drug loading and the dissolution rate of the drug-containing fibers can be tuned by over two orders of magnitude by varying the HPβCD/PVA ratio.

1. Introduction

Nanostructured materials that respond to stimuli such as temperature, pH, and humidity are of great interest to enable targeted drug delivery,[1–9] particularly of compounds with low aqueous solubility. Materials that are responsive to changes in humidity may be useful for oral transmucosal delivery (sublingual) applications for use in geriatric and pediatric patient care as well as for patients with difficulty swallowing or with the inability to produce sufficient saliva.[10,11] Sublingual delivery has typically involved fast dissolving/disintegrating drug delivery membranes (FDDMs) in a powder form that promotes rapid dissolution due to the high surface area. Nanofibers are an alternative to powders with several advantages such as an extraordinarily large surface area to mass ratio with a highly porous mat structure, which facilitates rapid dissolution.

Electrospinning is a simple and versatile method to produce polymer-based nanofibers.[12–15] Nanofibers can be produced from synthetic polymers such as polyvinylpyrrolidone, poly(ethylene oxide), and poly(vinyl alcohol) as well as natural biopolymers such as gelatin, collagen, and alginate (more exhaustive lists have been compiled elsewhere).[16,17] Moreover, the composition of nanofiber systems can be carefully selected to provide a range of dissolution rates (rapid, sustained, immediate, delayed, modified, *etc.*).[17,18] Nanostructured drug delivery systems that can enhance the dissolution of poorly water soluble (PWS) drugs are of particular interest and can be achieved by electrospinning drug-embedded nanofibers.[19–23] For example, Yu *et al.* reported the first such example by electrospinning ibuprofen loaded PVP filaments and illustrated the rapid release (<15 s) capabilities of nonwoven nanofiber mats.[10] However, incorporating a drug into a nanofiber mat does not ensure its delivery due to low drug loading or poor drug solubility and stability.

The use of complexing agents may address these issues. Incorporating the drug within an inclusion complex improves the aqueous solubility as well as the bioavailability.[24–39] Cyclodextrin (CD), donut shaped molecules made of 6, 7 or 8 membered α-D-glucopyranose rings (α, β or γ CD, respectively), are commonly used complexing agents as their hydrophobic cavity can host PWS drugs while the hydrophilic exterior can aid solubility.[36–40] While drug–CD complexes have been used to deliver drugs *via* multiple administration routes including oral, sublingual, ophthalmic, and transdermal,[31] the use of these complexes within electrospun polymer nanofibers is yet to be fully explored.

Cyclodextrins have been incorporated into nanofibers by blending them with an electrospinnable polymer.[41–43] Recently,

Department of Chemical and Biomolecular Engineering, North Carolina State University, Raleigh, NC 27695-7905, USA. E-mail: khan@eos.ncsu.edu; Tel: +1 919-515-4519

† Electronic supplementary information (ESI) available. See DOI: 10.1039/c3ra43836h

‡ Co-first authors.

§ Current address: Princeton University, Department of Chemical and Biological Engineering, Princeton, NJ 08544, USA.

¶ Current address: DuPont Central Research and Development, 200 Powder Mill Road, Wilmington, DE 19880-0304, USA.

the ability to electrospin small molecules, such as cyclodextrins, to produce uniform fibers has been reported.[44,45] Previously, we described the formation of hydroxypropyl-β-cyclodextrin (HPβCD) electrospun nanofibers without the addition of a carrier polymer *via* hydrogen bonding aggregation.[44] In this work, we have electrospun moisture-sensitive, supramolecular complexes of cyclodextrin, drug and poly(vinyl alcohol) (PVA), a water soluble electrospinnable polymer. The use of PVA serves two unique features: unlike other polymers it has no effect on the complexation of CDs with PWS drugs[40] and yet it plays a synergistic role in facilitating fiber formation. We can thus incorporate a high HPβCD content (as much as 90% per weight of fibers) to maximize the drug loading. Using ketoprofen as a model PWS drug known to form inclusion complexes with cyclodextrin, we show that the dissolution time can be tuned over two orders of magnitude by varying the fiber composition, *i.e.* the PVA content. These are promising materials for controlled release in sublingual drug delivery applications.

2. Materials and methods

Poly(vinyl alcohol) (Mowiol 40-88) was purchased from Sigma-Aldrich (205 kDa, 88% degree of hydrolysis), ketoprofen was purchased from MP Biomedical (Solon, OH), and hydroxypropyl-β-cyclodextrin (91.2% purity) was purchased from CTD, Inc (High Springs, FL, technical grade, product code THPB-T), and they were used without further purification. The choice of PVA molecular weight was based on its electrospinnability, as envisaged from our previous work.[12]

Electrospinning

The HPβCD and PVA stock solutions were prepared by combining appropriate amounts with deionized water and mixing in a shaker bath overnight at 35 °C and 60 °C, respectively. All solutions were stored at 4 °C. Various blends were prepared by combining appropriate proportions of stock solutions and mixing at 35 °C until homogenous. To load the model drug, a known mass of ketoprofen powder was added to the prepared blend solutions and mixed in a shaker bath.

The extent of drug loading was determined by known methods established to determine cyclodextrin phase-solubility.[46] Briefly, excess ketoprofen was blended with the desired PVA/HPβCD solution and the excess, undissolved powder was removed by syringe-filtering the sample. The ketoprofen content in the solution was then determined by UV-Vis absorbance spectrophotometry (Jasco V550). The presence of PVA and HPβCD was found not to affect the UV absorbance spectrum for ketoprofen.

For electrospinning, blends of HPβCD/PVA with and without ketoprofen were loaded into a syringe fitted with a stainless steel needle (0.508 mm i.d.) and attached to a power supply (Gamma High Voltage Research, D-ES-30PN/M692). A flow rate of 0.5 mL h^{-1}, a collecting distance of 12 cm, and an applied voltage of 5–11 kV were used, as previously described.[44]

Solution characterization

Viscosity measurements were performed at 25 °C on a TA Instruments® AR-2000 stress controlled rheometer using with a 4 cm, 2° cone and plate geometry. All rheological measurements were performed in triplicate to ensure reproducibility within ±5%. Surface tension measurements at the air–solution interface were made using the Wilhelmy plate method with a platinum rectangular thin blade. The electrical conductivity was measured using an EC meter (Fisher Accumet BASIC AB30).

Fiber analysis

For SEM analysis, the electrospun fibers were coated with gold and observed with a Hitachi S-3200 or FEI XL30 SEM. The average fiber diameter was determined by measuring the fiber diameters of at least 100 individual fibers from multiple SEM images using ImageJ software provided by NIH. Fourier transform infrared spectroscopy (FTIR) studies were performed using a Nicolet 6700 FTIR spectroscope (Thermo Electron Corp). Each spectrum was acquired with 256 scans with a resolution of 4 cm^{-1} and a spectral range of 4000–400 cm^{-1}. For calorimetry experiments, 8–12 mg of fibers were loaded and sealed in a hermetic aluminum pan. Calorimetry studies were done using a TA instruments® Q2000 Differential Scanning Calorimeter. The samples were heated from room temperature to 250 °C, held isothermally for 5 min, then cooled to room temperature, and reheated to 250 °C at a rate of 10 °C min^{-1}. The glass transition temperature was determined from the inflection point of the specific heat capacity of the second scan. X-ray diffraction studies were conducted using an X'Pert PRO Materials Research Diffractometer (PANalytical, Netherlands).

For the dissolution studies, approximately 5 mg of electrospun mat was placed in a beaker containing 25 mL of water. The dissolution was monitored by videotaping with a Canon EOS SLR Rebel SR1 in high resolution mode. The dissolution time was determined as the time where no discernible gel was left on the water surface.

3. Results and discussion

We began by electrospinning blends of PVA and HPβCD. Neat PVA (6 wt%) and HPβCD (70 wt%) (the concentrations were based on previous reports from our group[12,44]) could be electrospun to produce uniform nanofibers with diameters of 233 ± 33 nm and 996.7 ± 117.2 nm, respectively (Fig. 1a and f). We observed a decrease in the resulting fiber diameter with increasing PVA content, (Fig. 1b–e, Table 1, ESI Fig. 1b and 2†). To maximize the potential drug loading, we aimed to minimize the amount of PVA. Interestingly, adding relatively small amounts of PVA (0.1% w/w) to HPβCD (60% w/w) produced uniform bead-free fibers, despite the observation that the minimum concentrations required to produce uniform fibers from neat HPβCD and neat PVA were 70 wt% and 5 wt%, respectively. This is illustrated most clearly in Fig. 2, where the beads obtained from electrospinning HPβCD (60% w/w, Fig. 2a) transformed into microfibers upon the addition of a small amount of PVA (Fig. 2b). We believe that in the systems with

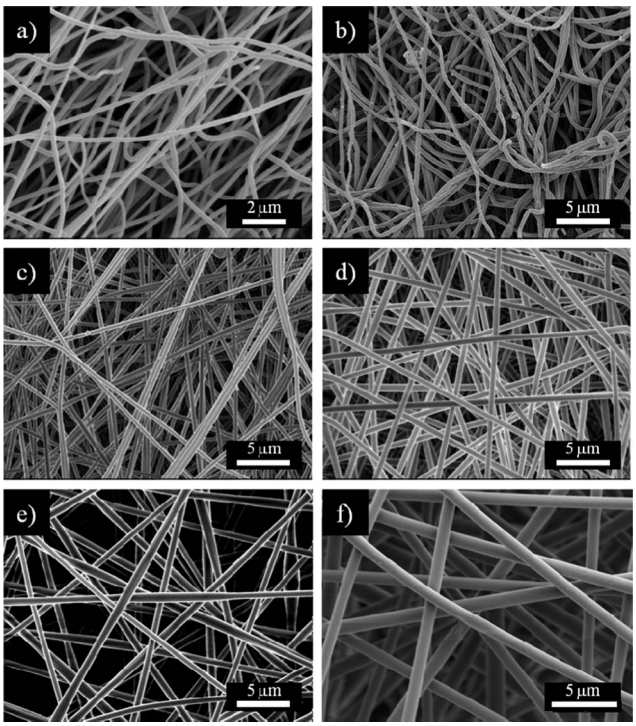

Fig. 1 SEM micrographs of the electrospun HPβCD/PVA blend fibers: (a) 0/100 (b) 30/70, (c) 50/50, (d) 70/30, (e) 90/10, and (f) 100/0 (HPβCD/PVA).

small amounts of PVA, fiber formation can be attributed to hydrogen bonding aggregation between HPβCD molecules facilitated by PVA, analogous to depletion flocculation. This result is consistent with our previous study of forming fibers from neat HPβCD, in which we showed that hydrogen bonding plays a dominant role in forming extensive networks of CD molecules *via* a mechanism akin to depletion flocculation and provides enough molecular cohesion to elongate and form fibers.[44]

The solution properties of the PVA/HPβCD system were analyzed to better understand why blending with PVA promotes fiber formation, even when the concentration is well below the entanglement concentration.[47] We compared systems that produced uniform fibers: neat PVA (6 wt%), neat HPβCD (70 wt %), and a blend (0.1/60 wt% PVA/HPβCD). The blends of HPβCD and PVA had higher solution conductivities compared to the neat HPβCD solution, as seen in Table 1 and in ESI

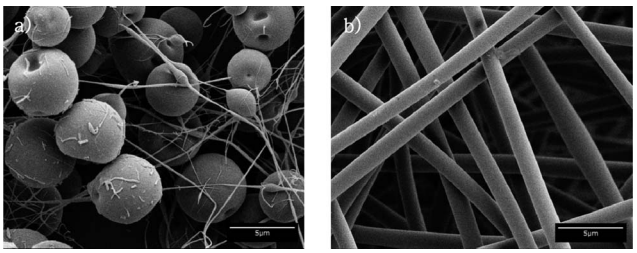

Fig. 2 Morphology of the mats electrospun from (a) 60 wt% HPβCD and (b) 60 wt% HPβCD/0.1 wt% PVA aqueous solutions.

Fig. 1.† While the increase in conductivity may contribute to the decrease in fiber diameter, it does not explain why blending enhanced fiber formation. The addition of PVA also significantly decreased the solution viscosity compared to the neat CD system; however, a decrease in viscosity does not generally facilitate fiber formation.[17] Therefore, other parameters must influence fiber formation.

We hypothesize that extended networks are forming between PVA and HPβCD, and aggregates may be responsible for stabilizing the electrospinning jet and aiding the formation of uniform fibers. The formation of these networks was probed by examining the solution rheology to analyze the impact of HPβCD addition on the polymer entanglement concentration (C_e) of PVA. The C_e was determined as the slope transition when plotting the specific viscosity ($\eta_{sp} = (\eta_o - \eta_s)/\eta_s$) as a function of polymer concentration, and it represents the concentration at which polymer chains start to overlap and interact with one another.[48] As seen in Fig. 3, the C_e of the neat PVA solution (2.5 w/w) decreased to 1.7, 1.1, and 0.8 w/w with the addition of 20, 30, and 40 wt% HPβCD. The decrease in the C_e indicates strong interactions between the materials, which facilitate fiber formation.[47] Cyclodextrins are known to interact with other cyclodextrin molecules *via* hydrogen bonding to form aggregates.[49] The formation of these aggregates between HPβCD and other molecules, including PVA, is possible.[50] Moreover, these interactions between HPβCD and the PVA chains might be responsible for the shift in C_e and the fiber formation at lower concentrations than is possible for either neat material. The ability of the addition of a small amount of PVA to facilitate nanofiber formation is consistent with our previous work in electrospinning neat HPβCD, which attributes the electrospinnability of neat HPβCD to a mechanism analogous to depletion flocculation.[44]

Table 1 Properties of PVA and PVA/HPβCD solutions and the resulting electrospun fibers

Solution (HPβCD/PVA)	Viscosity (cP)	Conductivity (μs cm^{-1})	Surface tension (dynes per cm)	Morphology	Fiber diameter (nm)
0/100	185 ± 7	195.2 ± 1.2	52.7 ± 0.7	Nanofibers	233 ± 33
30/70	195 ± 9	180.5 ± 1.5	53.5 ± 0.5	Nanofibers	345 ± 45
50/50	344 ± 10	183.1 ± 0.9	54.2 ± 0.8	Nanofibers	409 ± 41
70/30	554 ± 16	175.2 ± 1	54.5 ± 0.9	Nanofibers	634 ± 35
100/0	3250 ± 45	6.2 ± 0.4	58.0 ± 0.8	Nanofibers	986.7 ± 117.2
60/0.1 (>99% CD)	359 ± 25	8.3 ± 0.3	58.4 ± 0.9	Fibers	1325 ± 515.2

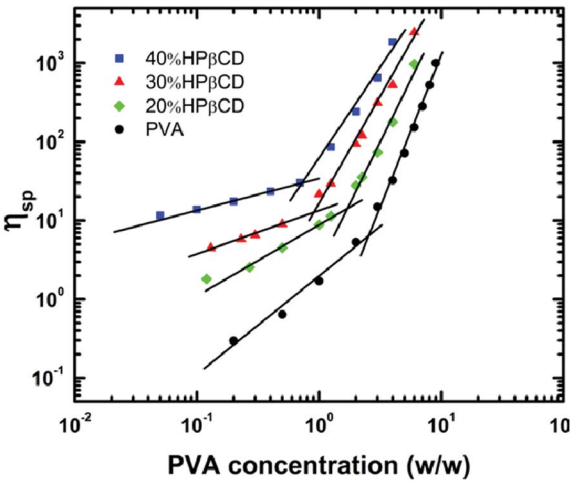

Fig. 3 Specific viscosity of aqueous solutions containing PVA and PVA/HPβCD blends.

Next, we examined electrospinning supramolecular complexes of HPβCD/PVA/ketoprofen. The amount of ketoprofen that can be dissolved or loaded into a solution increased with HPβCD content (Table 2). We found that the addition of ketoprofen, even up to 9% loading, had no appreciable effect on the fiber quality (Fig. 4), solution surface tension, or viscosity (ESI, Table 1†). At high ketoprofen loadings and high cyclodextrin content, we observed a decrease in fiber diameter, which can be attributed to the increase in solution conductivity upon addition of the ketoprofen. Yu *et al.* reported a similar increase in solution conductivity on the addition of ibuprofen to PVP solutions.[10]

We confirmed the presence of HPβCD/ketoprofen complexes in the fibers by FTIR. Fig. 5 shows the infrared spectra of the neat ketoprofen powder and the 50/50 HPβCD/PVA electrospun fiber mats with and without ketoprofen. Neat ketoprofen has two distinct peaks at 1697 and 1655 cm^{-1}, which are attributed to the carbonyl groups in the dimeric carboxyl acid and the ketonic groups, respectively.[51] The spectrum of the 50/50 HPβCD/PVA electrospun fiber mats contains two overlapping peaks at 1725 and 1740 cm^{-1}, which are attributed to the acetyl groups of PVA.[52] The spectrum of the ketoprofen loaded 50/50 HPβCD/PVA mats retains these overlapping peaks from the PVA, however the two carboxyl bands of ketoprofen are significantly reduced and possibly shifted from 1697 and 1655 cm^{-1}. This reduction and/or shift of the ketoprofen carbonyl groups indicates a change in the ketoprofen molecular interaction. This change may be due to a disruption of the ketoprofen intermolecular hydrogen bonding or the formation of an inclusion complex that shields the ketoprofen carboxyl groups, or a combination of both. Both types of interactions are

Table 2 Summary of dissolution times and ketoprofen loading of HPβCD blends. The dissolution time reported is the first time point at which gels were no longer visible on video recordings. Ketoprofen loading was determined using UV spectra

Blend ratio (HPβCD/PVA)	Dissolution time (s)	Ketoprofen loading (%)
0/100	462 ± 25	1.16 ± 0.09
30/70	520 ± 32	2.38 ± 0.11
50/50	415 ± 28	3.74 ± 0.12
70/30	180 ± 19	5.01 ± 0.11
90/10	10 ± 1.5	7.12 ± 0.15
100/0	~0.207	8.55 ± 0.10

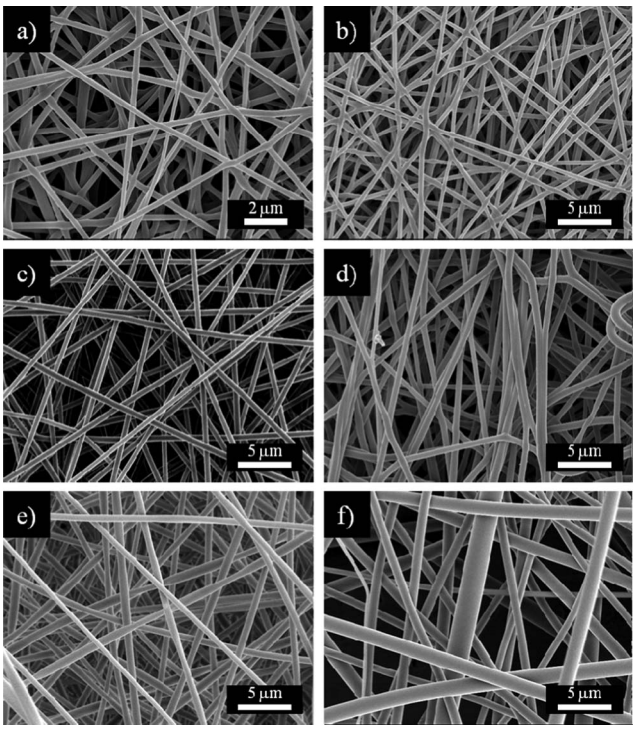

Fig. 4 SEM micrographs of electrospun ketoprofen loaded PVA/HPβCD blend fibers: (a) 0/100 (b) 30/70, (c) 50/50, (d) 70/30, (e) 90/10, and (f) 100/0 (HPβCD/PVA).

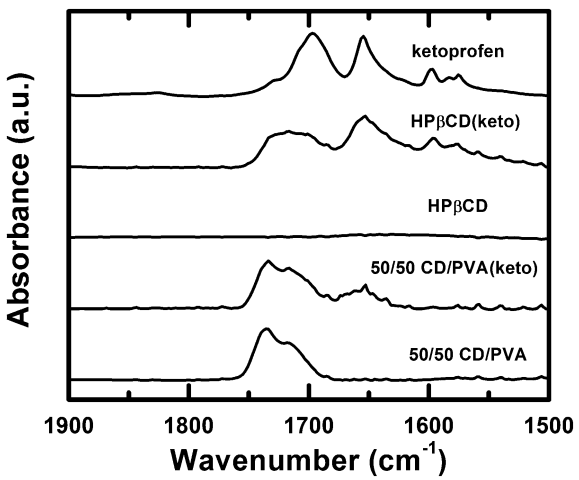

Fig. 5 Infrared spectrum of the ketoprofen carbonyl (C=O) stretching region for the neat and drug loaded HPβCD fibers and HPβCD/PVA blend fibers.

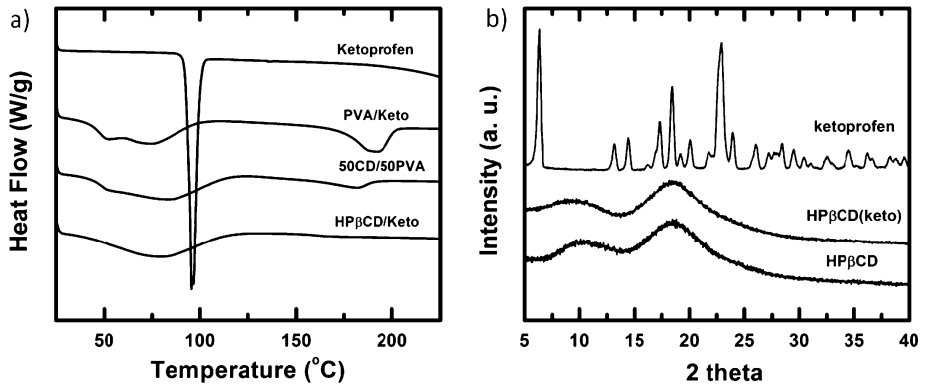

Fig. 6 The (a) DSC thermograms and (b) X-ray diffraction patterns for ketoprofen and the other materials as specified.

expected to disrupt the crystalline nature of ketoprofen and thus aid in rapid drug dissolution.[10]

Changes in the ketoprofen crystallinity upon fiber processing were examined using DSC and XRD. The DSC thermographs of the ketoprofen powder and the neat and ketoprofen loaded nanofibers are presented in Fig. 6a. As an amorphous blend, HPβCD/PVA does not exhibit any sharp peaks apart from a broad endotherm due to the dehydration of water. Ketoprofen, a crystalline drug, exhibits a single sharp endothermic response at approximately 94 °C. However, this distinct peak disappears when ketoprofen is loaded into the HPβCD/PVA mats. This indicates that ketoprofen is no longer a crystalline material, but is amorphously distributed in the fibrous mat, similar to previous reports.[10] Moreover, the XRD diffraction pattern of neat ketoprofen displays numerous peaks that are indicative of a crystalline material (Fig. 6b). These peaks disappear when ketoprofen is incorporated into a fibrous mat, further supporting the presence of an amorphously distributed drug.[10]

Finally, we examined the dissolution of the HPβCD and HPβCD/PVA blends with and without ketoprofen. The HPβCD/ketoprofen complex fibers were extremely responsive to moisture, and disintegrated and dissolved almost immediately as each part of the mat made contact with the water surface. By videotaping the dissolution and performing frame by frame analysis, we estimated that a 1″ square of nanofibers completely dissolved in 0.207 s, as seen in ESI Fig. 3.†

Interestingly, the addition of PVA slowed the dissolution of the membranes, despite the decrease in fiber size (Table 2). The increase in dissolution time appears to be directly proportional to the amount of PVA up to 70% PVA. With further increases in PVA content, the dissolution rate decreased slightly, which may indicate that both the solubility and fiber size affect the dissolution rates. Nevertheless, the dissolution time can be tuned over two orders of magnitude by varying the fiber composition, *i.e.* the PVA loading. Further explorations of the dissolution rates in various environments (*e.g.* pH, enzymes that mimic saliva, *etc.*) are needed.

Because ketoprofen was shown to be amorphously distributed within the fiber, it is believed that the total disintegration and dissolution of the fibers led to the complete release of the drug contained within. These results indicate that it is advantageous to create fibers with the highest possible HPβCD content, not the smallest fiber diameter, to release the maximum amount of drug in the shortest time.

4. Conclusions

We have electrospun moisture-sensitive fibers from supramolecular complexes of PVA/HPβCD/ketoprofen for potential sublingual drug delivery applications. Blending the two components appears to enhance PVA entanglement, which facilitated fiber formation. We attribute the enhancement of PVA entanglement to the molecular interactions of the cyclodextrin, which leads to networks of HPβCD aggregates and PVA chains that are analogous to depletion flocculation. The effect of fiber size on the dissolution rates was examined by varying the amount of PVA in the electrospinning solution. The fiber diameter decreased with increasing PVA content due to increases in the solution conductivity, but the drug loading and dissolution rates increased with decreasing PVA content. Consequently the PVA content could be used to modulate the drug amount and release time, with fibers having the highest HPβCD content releasing the most drug in the shortest amount of time.

References

1 A. Tiwari, M. Ramalingam, H. Kobayashi, and A. Turner, *Biomedical Materials and Diagnostic Devices*, WILEY-Scriverner, Hoboken, NJ, 2012.
2 A. Tiwari, *Polysaccharides: Development, Properties and Applications*, Nova Science Publishers, Inc., Hauppauge, NY, 2010.
3 A. Tiwari and H. Kobayashi, *Responsive Materials and Methods*, WILEY-Scriverner, Hoboken, NJ, 2013.
4 S. Shukla, Vamakshi, Minakshi, A. Bharadavaja, A. Shekhar and A. Tiwari, *Adv. Mater. Lett.*, 2012, **3**, 421–425.
5 A. Tiwari, *Adv. Mater. Lett.*, 2013, **4**, 507–507.
6 Y. Sharma, A. Tiwari, S. Hattori, D. Terada, A. Sharma, M. Ramalingam and H. Kobayashi, *Int. J. Biol. Macromol.*, 2012, **51**, 627–631.

7 A. Tiwari, Y. Sharma, S. Hattori, D. Terada, A. Sharma, A. Turner and H. Kobayashi, *Biopolymers*, 2012, **99**, 334–341.
8 G. Verma and P. Hassan, *Phys. Chem. Chem. Phys.*, 2013, **15**, 17016–17028.
9 M. Mortonov, Y. Roiter, I. Tokarev and S. Mink, *Prog. Polym. Sci.*, 2010, **35**, 174–211.
10 D. G. Yu, X. X. Shen, C. Branford-White, K. White, L. M. Zhu and S. W. A Bligh, *Nanotechnology*, 2009, **20**, 55104–55112.
11 Y. R. Fu, S. C. Yang, S. H. Jeong and K. Park, *Crit. Rev. Ther. Drug Carrier Syst.*, 2004, **21**, 433–475.
12 C. Tang, C. D. Saquing, J. R. Harding and S. A. Khan, *Macromolecules*, 2010, **43**, 630–637.
13 S. Talwar, J. Hinestroza, B. Pourdeyhimi and S. A. Khan, *Macromolecules*, 2008, **41**, 4275–4283.
14 C. D. Saquing, J. L. Manasco and S. A. Khan, *Small*, 2009, **5**, 944–951.
15 C. A. Bonino, K. Efimenko, S. I. Jeong, M. D. Krebs, E. Alsber and S. A. Khan, *Small*, 2012, **8**, 1928–1936.
16 J. D. Schiffman and C. L. Schauer, *Polym. Rev.*, 2008, **48**, 317–352.
17 A. L. Andrady, *Science and Technology of Polymer Nanofibers*, John Wiley and Sons Inc., Hoboken, NJ, 2008; p. 403.
18 F. Ignatious, L. H. Sun, C. P. Lee and J. Baldoni, *Pharm. Res.*, 2010, **27**, 576–588.
19 E. R. Kenawy, G. L. Bowlin, L. Mansfield, J. Layman, D. G. Simpson, E. H. Sanders and G. E. Wnek, *J. Controlled Release*, 2002, **81**, 57–64.
20 M. Goldberg, R. Langer and X. Q. Jia, *J. Biomater. Sci., Polym. Ed.*, 2007, **18**, 241–268.
21 E. R. Kenawy, F. I. Abdel-Hay, M. H. El-Newehy and G. E. Wnek, *Mater. Sci. Eng., A*, 2007, **459**, 390–396.
22 K. Kim, Y. K. Luu, C. Chang, D. F. Fang, B. S. Hsiao, B. Chu and M. Hadjiargyrou, *J. Controlled Release*, 2004, **98**, 47–56.
23 S. Agarwal, A. Greiner and J. H. Wendorff, *Adv. Funct. Mater.*, 2009, **19**, 2863–2879.
24 T. Loftsson, D. Hreinsdottir and M. Masson, *Int. J. Pharm.*, 2005, **302**, 18–28.
25 E. M. M. Del Valle, *Process Biochem.*, 2004, **39**, 1033–1046.
26 R. Romi, P. L. Nostro, E. R. Bocci and P. Baglioni, *Biotechnol. Prog.*, 2005, **21**, 1724–1730.
27 H. J. Buschman, U. Denter, D. Knittel and E. Schollmeyer, *J. Text. Inst.*, 1998, **89**, 554–561.
28 B. Voncina, V. Vivod and D. Jausovec, *Dyes Pigm.*, 2007, **74**, 642–646.
29 M. Tanaka, H. Matsuda, H. Sumiyoshi, H. Arima, F. Hirayama, K. Uekama and S. Tsuchiya, *Chem. Pharm. Bull.*, 1996, **44**, 416–420.
30 M. E. Brewster and T. Loftsson, *Adv. Drug Delivery Rev.*, 2007, **59**, 645–666.
31 M. E. Davis and M. E. Brewster, *Nat. Rev. Drug Discovery*, 2004, **3**, 1023–1035.
32 A. Magnusdottir, M. Masson and T. Loftsson, *J. Inclusion Phenom. Macrocyclic Chem.*, 2002, **44**, 213–218.
33 R. A. Rajewski and V. J. Stella, *J. Pharm. Sci.*, 1996, **85**, 1142–1169.
34 J. Pitha, T. Irie, P. B. Sklar and J. S. Nye, *Life Sci.*, 1988, **43**, 493–502.
35 K. Uekama, *J. Pharm. Soc. Jpn.*, 2004, **124**, 909–935.
36 T. Loftsson and D. Duchene, *Int. J. Pharm.*, 2007, **329**, 1–11.
37 T. Irie and K. Uekama, *J. Pharm. Sci.*, 1997, **86**, 147–162.
38 T. Loftsson and M. E. Brewster, *J. Pharm. Sci.*, 1996, **85**, 1017–1025.
39 H. Matsuda and H. Arima, *Adv. Drug Delivery Rev.*, 1999, **36**, 81–99.
40 T. Loftsson and M. Masson, *J. Drug Delivery Sci. Technol.*, 2004, **14**, 35–43.
41 T. Uyar and F. Besenbacher, *Eur. Polym. J.*, 2009, **45**, 1032–1037.
42 T. Uyar, Y. Nur, J. Hacaloglu and F. Besenbacher, *Nanotechnology*, 2009, **20**, 125703.
43 F. Kayaci and T. Uyar, *Food Chem.*, 2012, **133**, 641–649.
44 J. Manasco, C. Saquing, C. Tang and S. Khan, *RSC Adv.*, 2012, **2**, 3778–3784.
45 A. Celebioglu and T. Uyar, *Langmuir*, 2011, **27**, 6218–6226.
46 P. Mura, G. P. Bettinetti, A. Manderioli, M. T. Faucci, G. Bramanti and M. Sorrenti, *Int. J. Pharm.*, 1998, **166**, 189–203.
47 M. G. McKee, G. L. Wilkes, R. H. Colby and T. E. Long, *Macromolecules*, 2004, **37**, 1760–1767.
48 S. Shenoy, W. Bates, H. Frisch and G. Wnek, *Polymer*, 2005, **46**, 3372–3384.
49 O. Hausler and C. C. Mullergoymann, *Starch/Staerke*, 1993, **45**, 183–187.
50 Y. He, P. Fu, X. Shen and H. Gao, *Micron*, 2008, **39**, 495–516.
51 D. Yu, C. Branford-White, X. Shen, X. Zheng and L. Zhu, *J. Dispersion Sci. Technol.*, 2010, **31**, 902–908.
52 V. C. Costa, H. S. Costa, W. L. Vasconcelos, M. Pereira, R. Oréfice and H. S. Mansur, *Mater. Res.*, 2007, **10**, 21–26.